PERGAMON

Continental Shelf Research 19 (1999) 821–842

CONTINENTAL SHELF RESEARCH

Storm-related sea level variations along the North Sea coast: natural variability and anthropogenic change

H. Langenberg[a,*], A. Pfizenmayer[a], H. von Storch[a], J. Sündermann[b]

[a]*GKSS Research Centre, Max-Planck Str., 21502 Geesthacht, Germany*
[b]*Zentrum für Meeres- und Klimaforschung der Universität Hamburg, Troplowitzstr. 7, 22529 Hamburg, Germany*

Received 11 November 1997; received in revised form 9 July 1998; accepted 19 October 1998

Abstract

The influence of a changing wind climate on the sea surface elevations along the North Sea coast was investigated, with a statistical down-scaling technique and with a dynamical model. Firstly, in an analysis of past variability the two models were run for different periods: the numerical model for the winters 1955–1993 and the statistical one for the winters 1899–93. Secondly, a fine-scale time slice experiment for a control run and a scenario for doubled atmospheric carbon dioxide concentration was used (in both the dynamical and the statistical down-scaling model) to assess the sea level related changes due to an (anthropogenic) increase in atmospheric carbon dioxide concentration. Both models agree on the following results: (a) In the past, the winter means of high water levels along the North Sea coast increase on the order of 1–2 mm/yr, on account of only the atmospheric forcing; (b) the high intramonthly percentiles – reduced by the winter averages – show no clear trend; and (c) the British Coast exhibits a slight negative and the continental coast an equally small positive tendency. In the climate scenarios, the effect on the high percentiles follows the same pattern. A slightly larger and everywhere positive difference is diagnosed in the mean water levels along the North Sea coast. Together with the hindcast result, the above interpretations might suggest a continuing increase of mean water levels at the North Sea coast due to an increasing CO_2 concentration in the atmosphere; this would occur throughout the second half of this century and, possibly, beyond. The high frequency variability appears to be much less affected. However, the natural variability of the system is too strong to clearly identify such a process, or attribute it to anthropogenic development. This study evaluates the impact of a changing atmospheric forcing only. Additional influences, such as the eustatic and isostatic effects, are not taken into account.

*Corresponding author. Fax: + 44 171 843 4596; e-mail: langenberg@gkss.de.

0278–4343/99/$ – See front matter
PII: S0278–4343(98)00113–7

1. Introduction

In recent years, there has been considerable concern expressed about the possible effects of (anthropogenic) climate change, on living conditions in coastal areas. One aspect of this anxiety has been the question of whether or not an increase in storminess, thereby an increase in extreme water levels, is to be expected or has already been observed.

Several studies (e.g. Rohde, 1992; Führböter et al., 1988) have pointed out that, in the North Sea, an increase in the height of storm surges has indeed been recorded in the past. It is often concluded that, due to the ongoing emission of greenhouse gases into the atmosphere – which is held responsible for the observed changes – this tendency is going to continue or even accelerate.

However, from the observations available it is difficult to distinguish between the effects of the multitude of factors – other than meteorology – that have an influence on sea levels e.g. construction works, land sinking or rising and similar non-climate related changes. Here, by using models that take into account only clearly defined effects, it is possible to extract the storm-related component of sea level changes. Thus, the question arises whether it is indeed the storm-related component that has induced the observed increasing storm surge heights.

It should be noted that the thermal expansion of the oceans – a climate-related factor that is important for the past development – is neither accounted for in the models, nor is the subject of this investigation.

In the first part of the present study, a 39 year hindcast of the sea surface elevations along the North Sea coast is used to assess the trends and changes in extreme and in mean water levels due to changes in the atmospheric forcing. The results from this exercise are also used in the analysis of the climate change scenarios for an estimate of the natural variability of the system.

The observed sea surface pressure fields from the Det Norske Meteorologisk Institutt (DNMI) used to force the dynamical model, suffer from a decisive drawback: after the year 1982 the method of analysis was changed from a manual analysis to numerical weather prediction systems and, simultaneously, the area covered by the analysis was changed. Additionally, creeping inhomogeneities from an increasing number of observations might be present in the data set. In order to account for the first inhomogeneity the two sections of data before and after 1982 were analysed independently, however, no significant effect on the water levels was found. With regard to the second inhomogeneity, Gunther et al. (1998) rated the impact to be small in areas where data were available throughout the whole period – a condition that holds for the North Sea.

In the statistical model, an independent data set of monthly mean air pressure maps from different weather services are used; They are believed to be mostly homogeneous (Trenberth and Paolino, 1980).

In the second part of the paper the hindcast is complemented by the exploitation of two high-resolution (T106 $\sim$ 100 km) atmospheric GCM (ECHAM3) scenarios: a control run with a climate comparable to present day conditions together with a "$2 \times CO_2$" run associated with an enhanced greenhouse effect. These so called time-slice

experiments use the sea surface temperature distributions and sea ice distributions from a present day climatology as a lower boundary condition for the control run and their changes, due to doubled atmospheric carbon dioxide concentration, as simulated in a long-term run of a coarse-grid coupled ocean–atmosphere model (Cubasch et al., 1992) as the lower boundary, condition for the "$2 \times CO_2$" run.

Both versions are integrated over 6 years (Cubasch et al., 1995). The results have directly been analysed by various authors (e.g. Bengtsson et al., 1995; Cubasch et al., 1996; Beersma et al., 1997), each with a different emphasis. The control run has generally been found to represent present climate reasonably well. Regarding mid-latitude storminess, Beersma et al. (1997) show that the differences between the control run and the doubled carbon dioxide concentrations are relatively small.

Von Storch and Reichardt (1997) – based upon the same ECHAM3 time-slice experiments – use a statistical down-scaling method that is similar to the one presented here. These investigators find no significant difference between the control and "$2 \times CO_2$" scenario.

Flather and Smith (1998) – who use the same GCM scenarios as meteorological forcing in their storm surge model and calculate the height of a "5 year surge" – also come to the conclusion that the increase in the "$2 \times CO_2$" scenario, compared to the control run, is not statistically significant in the light of the high natural variability of the system.

Here, additional information is gained in the analysis by the comparison of the two types of models that are based on different philosophies. The dynamical storm surge model seeks to incorporate the dynamics of the ocean and, thus, to react flexibly to changes in the atmosphere–ocean interaction. The empirical model analyses statistical correlations between certain atmospheric pressure patterns and the corresponding patterns of the water levels, within a fitting interval; it extrapolates this relationship in the time domain. The latter procedure works remarkably well, whenever there is a persistent physical connection between parameters throughout the time of the investigation; however, it must break down when a change in the forcing-response dynamics occurs.

For the assessment of climate change – where the condition of a persistent physical connection might well be violated – it is thus interesting to complement the statistical technique with a dynamical one. From the difference in accuracy of the statistical model in the present climate and under doubled atmospheric CO_2-concentrations, an indication can be gained as to whether or not such a change in the dynamics occurs.

Also, running a dynamical model is by far more expensive in terms of computational costs. Proving that the statistical relationship, on which the empirical model is based, still holds in changing climate conditions allows the fast and efficient evaluation of future – longer and more accurate – GCM climate change scenarios.

In Sections 2–5 the two models are introduced, validated and evaluated in parallel. Sections 6 and 7 are devoted to the comparison of the results and conclusions are drawn from the differences and similarities that have emerged.

2. The models

In this Section, the two models are introduced and their input data are described. Their set-ups differ decisively: the statistical down-scaling model runs at rather low expense and requires only very coarse parameters (here: monthly mean atmospheric pressure fields, on a 5° grid) as atmospheric input data; additionally, it requires several years of sea level observations for each tide gauge that is to be simulated. Thus, for the analysis of the past (Section 4) the observations at the tide gauges are analysed directly: only for the extrapolation to the climate scenarios is the statistical model utilised.

The dynamical storm surge model is more expensive and needs an atmospheric input on a finer scale (here: $\Delta x = 100$ km and $\Delta t = 12$ h), but delivers data at each grid point without a prerequisite of observations. Such forcing data are only available for the years 1955–1993, so that the simulation of the past is limited to this period.

2.1. The dynamical storm surge model

The dynamical storm surge model is a shelf sea circulation model based upon the primitive equations, of the Northwestern European Shelf, the North Sea and the Baltic Sea. It covers the area from 47° 35′ N to 65° 47′ N and from 15° 5′ W to 30° 5′ E (see Fig. 1), with a grid size of 6′ in meridional direction and 10' in zonal direction and a time step of 10 min. The semi-implicit numerical scheme has been developed by Backhaus (1985) and has been used in various three-dimensional applications (e.g. Hainbucher et al., 1987). Since for storm surge simulation a two-dimensional approach was found to be sufficient from various sensitivity studies and in view of the rather long integration time required, the model was modified to a vertically integrated version.

Three-dimensional climatological monthly mean fields of temperature and salinity (Damm, 1989; Tomczak and Goedecke, 1962) are used to determine the baroclinic pressure gradients between the grid boxes, so that the difference in sea surface elevation due to the density difference between the North Atlantic and the German Bight is taken into account climatologically. The same density fields are used for the climate scenarios, so that (for instance) the effect of thermal expansion is not taken into account.

At the open boundaries, sea surface elevations from eight partial tides ($Q_1, O_1, P_1, K_1, N_2, M_2, S_2, K_2$) are prescribed; one month of spin-up time is allowed, in order to let the tides propagate throughout the model area.

Wind stress, as well as atmospheric pressure, are prescribed at the sea surface. The procedure of wind stress calculation varies, depending upon the available data: for the 39 year hindcast with DNMI-data, only atmospheric pressure fields are available. The wind stress is then calculated with an approach by Luthardt and Hasse (1983), which was especially designed to calculate wind stress from atmospheric pressure fields in potential high wind speed situations. The DNMI changed its methods of observation in 1982, so that the data set is not homogeneous.

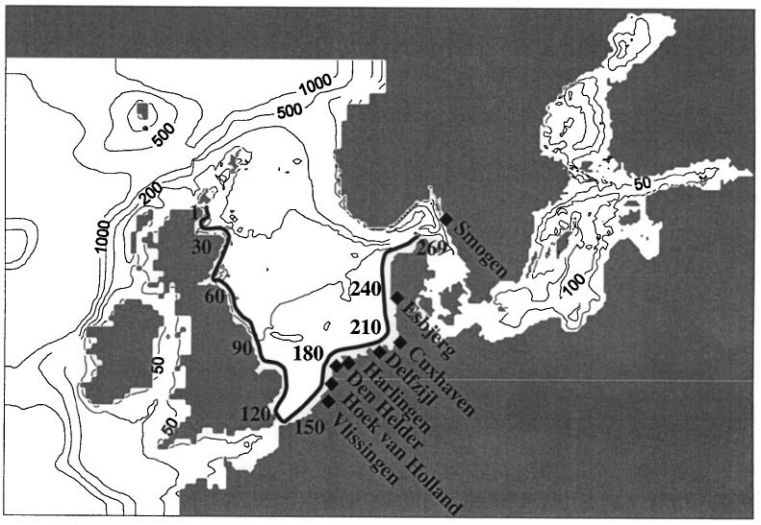

Fig. 1. Bathymetry of the model area. The black line connects every 30th point of the coastal vector (used for evaluation). The diamond marks indicate tide gauge positions.

Inhomogeneities are believed to be present, mainly in regions where data are notoriously sparse – thus excluding the well-observed North Sea (see, for example Günther et al., 1998). The area covered by the observations was also changed, however, so that for the very southeastern part of the Baltic Sea the DNMI data had to be complemented with ECMWF reanalyses. The two data fields were merged into each other at the boundary of the DNMI data with an interpolation scheme, but generally, consistency was very good so that no major adjustments had to be made.

For the scenarios from the GCM - run, sea surface winds (in 10 m height) are also available. Here, the approach adopted by Smith and Banke (1975) for the calculation of wind stress from sea surface winds was applied. Both methods for the calculation of the wind stress were found to give similar results, in a high wind speed test case.

The dynamical model simulates the water level in a grid box, whereas the tide gauge represents a point observation on the coast line. The water level in the nearshore area is far from uniform; therefore, the grid box water level and the *in situ* water level deviate. To account for this difference, an empirical correction of the model results is derived for those tide gauges for which data are available; this correction is piecewise linear/quadratic. As a typical example of the quality of correction, the scatter of simulated grid-box water levels and recorded in situ water levels are displayed, together with the linear/quadratic fit, in Fig. 2.

2.2. The statistical model

We use a statistical technique, similar to the one developed by von Storch and Reichardt (1997) that allows for the backward reconstruction of time series of

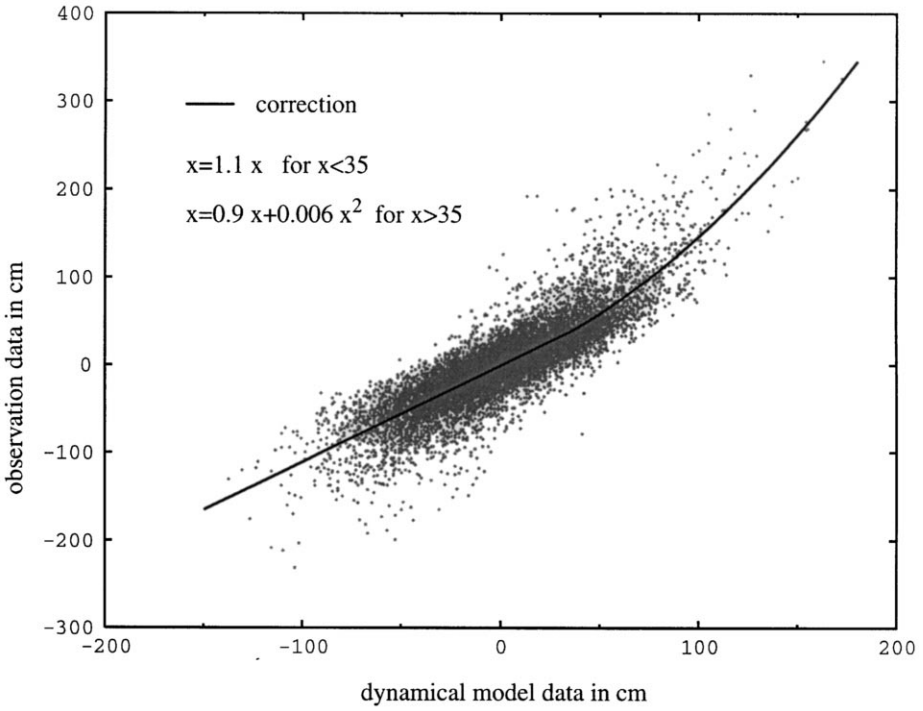

Fig 2. Scatter of pairs of simulated (horizontal axis) and observed (vertical axis) water levels at Cuxhaven (set Fig. 1), together with a piecewise linear/quadratic fit used for correcting the simulated data. The annual winter mean is subtracted from both the data sets.

intramonthly percentiles of some local variable, together with the construction of scenarios for these intramonthly percentiles consistent with a given global climate change scenario. The basic concept was to first build a statistical model that links the intramonthly percentiles to planetary scale monthly mean air-pressure (or other) fields, then to utilise this link to derive estimates of intramonthly percentiles (from historical monthly mean air-pressure maps, or from air-pressure field changes simulated in climate change scenarios).

2.2.1. The data

The base model deviates from the technique used by von Storch and Reichardt (1997), through the use of *redundancy analysis*, instead of canonical correlation analysis; this is applied to eight locations along the southern and eastern coast of the North Sea: Vlissingen, Hoek van Holland, Den Helder, Harlingen and Delfzijl along the Dutch coast; Cuxhaven for the German coast; Esbjerg in Denmark; and Smogen at the Swedish coast (Fig. 1). As a rule, these time series cover more than 100 years and are available twice daily. The tide gauges at Harlingen and Den Helder have been

significantly affected by the closing of the Ijsselmeer in the 1930s. A rough correction has been applied to this end. For sea level pressure (SLP) we used monthly analyses of observations over the Northern North Atlantic and Western Europe (70°W–20°E, 30°–70°N), for the years 1900–1996. This data set from the National Center for Atmospheric Research (NCAR) is mostly homogeneous and has a resolution of $5° \times 5°$. The NCAR data are too coarse to be used reasonably in the dynamical model; however in contrast to the DNMI data set, they are available over a long time period – a prerequisite for the statistical model. Therefore, the two models are forced with different atmospheric fields.

The daily in situ water level data reflect not only storm-related variations, but also the effect of various other processes as, for instance:

- the rise of the mean sea level because of the thermal expansion of water and the melting of glaciers (approximately 10–15 cm for the German Bight in the last century e.g. De Ronde and De Ruijter (1987));
- land sinking (the southern coast of the area) and rising (eastern coast);
- changes in the tidal dynamics, because of a changed morphology of the coastline (embankments, deepened estuaries);
- annual and nodal tidal cycles.

Because, in the present study, we are interested only in those variations of water level statistics that may be ascribed to changes in the atmospheric forcing, we have to discriminate between atmosphere-related variations and other effects. We do this by assuming that the atmosphere-related variations mostly take place on time-scales of less than one month, whereas the other processes have an impact on longer time-scales. This does not mean that there are no long-term influences of the atmosphere on water levels, but that the variability is largest on the short scale. Therefore, we isolate the slow, not atmosphere-related processes, by the subtraction of a long-term mean or trend from the data set. Here, we used a 5 year running mean of high water, and – for comparison with the dynamic model – the winter mean from November to March.

2.2.2. *The regression model*

A regression model was built which relates two sets of random vectors, $\mathbf{S}_t$ and $\mathbf{Q}_t$. In the present cases, the vector time series $\mathbf{S}_t$ represents the winter (NDJFM) monthly mean air-pressure (SLP) distributions. The other vector time series, $\mathbf{Q}_t$, is formed by the 50, 80, 90 and 97% intra-monthly quantiles of high water at different locations (Vlissingen (1), Hoek van Holland (2), … , Smogen (8)):

$$\mathbf{Q}_t = \begin{pmatrix} q_{50\%,1} \\ q_{80\%,1} \\ q_{90\%,1} \\ q_{97\%,1} \\ q_{50\%,2} \\ \vdots \\ q_{97\%,8} \end{pmatrix}_t . \tag{1}$$

Both vectors are centred, i.e. their time means are subtracted prior to the analysis. Also, a data compression with the help of EOFs (von Storch and Frankignoul, 1997) is done prior to the analysis, in order to avoid artificially enhanced correlations. Five EOFs are used for SLP and three for the intra-monthly percentiles.

A redundancy analysis (RDA) (Tyler, 1982; von Storch and Zwiers, 1998) is performed with the two vector time-series. The result of an RDA are pairs of vectors ($\mathbf{p}^{s;k}$, $\mathbf{p}^{q;k}$) and time coefficients $\alpha_{s;K}(t)$ and $\alpha_{q;k}(t)$, so that

$$\mathbf{S}_t = \sum_{k=1}^{K} \alpha_{s;k}(t)\,\mathbf{p}^{s;k}, \tag{2}$$

$$\mathbf{Q}_t = \sum_{k=1}^{K} \alpha_{q;k}(t)\,\mathbf{p}^{q;k} \tag{3}$$

The patterns $\mathbf{p}^{s;k}$ and $\mathbf{p}^{q;k}$ are determined such that the regressed expansion

$$\hat{\mathbf{Q}}_t = \sum_{k=1}^{K} \rho_k \alpha_{s;k}(t)\,\mathbf{p}^{q;k} \tag{4}$$

describes a maximum of variance of $\mathbf{Q}$, for a given number K. In order to have uniquely determined solutions, the expansion patterns $\mathbf{p}^{q;k}$ of the *predictand* are requested to be orthonormal, whereas the patterns $\mathbf{p}^{s;k}$ are requested to be linearly independent. The first pair of patterns is chosen so that a maximum of $\mathbf{Q}$-variance is explained; the second, so that a maximum of additional variance is represented (because of the orthonormality of the $\mathbf{p}^{q,k}$-patterns, the variance contributions in Eq. (4) may simply be added.) The coefficients are obtained by the projections

$$\alpha_{s;k} = \mathbf{S}^{\mathrm{T}}\mathbf{p}_A^{s;k}, \tag{5}$$

$$\alpha_{q;k} = \mathbf{Q}^{\mathrm{T}}\mathbf{p}^{q;k}, \tag{6}$$

where $\mathbf{p}_A^{s;k}$ are the adjoints to the patterns $\mathbf{p}^{s;k}$. In Eq. (6) the patterns $\mathbf{p}^{q;k}$ appear, since these are constructed to be orthonormal and thus self-adjoint. The patterns $\mathbf{p}^{s;k}$, on the other hand, are not orthonormal and therefore not self-adjoint.

The coefficients are normalized to one

$$\mathrm{Var}(\alpha_{q;k}) = \mathrm{Var}\,(\alpha_{s;k}) = 1$$

so that the three components of $\mathbf{p}^{q;k}$ may be interpreted as anomalies which occur typically together with the "field distribution" $\mathbf{p}^{s;k}$.

The down-scaling model, which relates the large-scale air-pressure information to the intra-monthly water level height, is a regression model $\alpha_{q;k} = \rho_k \alpha_{s;k}$ for the RDA-coefficients $\alpha_{s;k}$ and $\alpha_{q;k}$. A reconstruction in the 32-dimensional space (four quantiles

of eight stations) is then obtained using Eq. (3):

$$\mathbf{Q}_t = \begin{pmatrix} q_{50\%,1} \\ q_{80\%,1} \\ q_{90\%,1} \\ q_{97\%,1} \\ q_{50\%,2} \\ \vdots \\ q_{97\%,8} \end{pmatrix}_t = \sum_{k=1}^{K} \rho_k \alpha_{s;k}\,(t)\ \mathbf{p}^{q;k}. \tag{7}$$

The regression model (7) may be applied to anomalies of observed or simulated air pressure fields $\mathbf{S} = \sum \alpha_{s;k} \mathbf{p}^{s;k}$.

The redundancy analysis is undertaken with data collected from 1960 to 75. The first two redundancy pairs are shown in Fig. 3.

The first pair dominates; it describes more than three quarters of the explained variance and the time-coefficients are correlated with 0.86. The first percentile pattern exhibits the same sign for all stations and percentiles; the highest values are associated with the coast of the German Bight, with decreasing values toward the northern and southern parts of the examined area. The ranking of percentiles shows higher values for higher percentiles. This pattern of percentiles is associated with an SLP pattern that consists of a high-pressure system over Scandinavia and a low-pressure system north of the Azores. When such an SLP pattern prevails, the climatological westerly winds are weakened, so that the region experiences a more stable situation, thus less frequent and less intense synoptic disturbances, i.e. storms. The argument is linear, so that the pattern with a negative sign represents a situation with an intensified westerly mean flow, in which more storms are embedded.

The second pattern is characterized by a low-pressure system over the central North Atlantic with a weak pressure gradient over the North Sea. It is associated with increased monthly mean water levels and reduced higher percentiles. A similar pattern was found by von Storch and Reichardt (1997) for Cuxhaven, who argued that such an SLP pattern would push more water into the North Sea, but fewer storms are directed into the North Sea area.

The down-scaling model uses the first three RDA pairs, i.e., $K = 3$ in Eq. (7). The second and, particularly the third pair, improve the skill only slightly; however, more degrees of freedom for the evaluation of the time-slice scenarios are gained.

3. Validation

Both models are validated with the help of observations at various tide gauges (see Fig. 1). As the analysis will be based mainly on the intramonthly 90% quantiles and winter means of the high water levels, it is these quantities on which the validation is focussed. The 90% quantiles from both models can be compared directly to the observations. The observed winter means, however, contain a large increase that is not due to changes in the atmosphere; thus this cannot be simulated with the

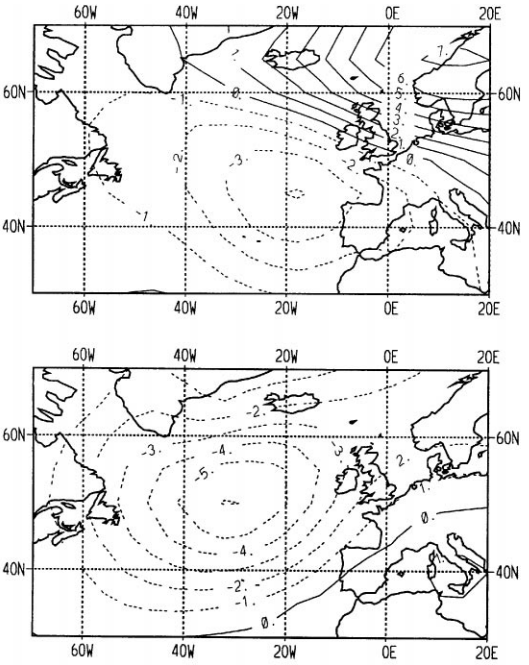

Quantile	50%	80%	90%	97%
Smogen	-10	-11	-12	-13
Esbjerg	-17	-22	-24	-28
Cuxhaven	-18	-23	-29	-38
Delfzijl	-14	-21	-26	-33
Harlingen	-16	-20	-24	-31
Den Helder	-12	-16	-19	-23
H.v.Holland	-10	-14	-17	-21
Vlissingen	-9	-10	-12	-16

Quantile	50%	80%	90%	97%
Smogen	6	5	4	3
Esbjerg	10	8	5	1
Cuxhaven	9	6	-1	-11
Delfzijl	7	4	-1	-13
Harlingen	8	5	-1	-11
Den Helder	6	4	0	-9
H.v.Holland	5	3	-1	-8
Vlissingen	4	2	0	-4

Fig. 3. First two pairs of redundancy patterns of observed winter (NDJFM) percentiles of the high water in cm (right) and simultaneous SLP (hPa) in the North Atlantic sector (left). Top (first pair): The correlation between the time coefficients is 0.88. The percentile pattern explains 79% of the variance. Bottom (Second pair): The correlation between the time coefficients is 0.34. The percentile pattern explains 7% of the variance.

presented models. Because of this difficulty in the case of winter means, the results from the two models are compared.

3.1. Dynamical model

Hourly observed data from the tide gauge in Cuxhaven were used for a first validation of the model output. The correlation between simulated and observed time-series amounts to 0.96 with a represented variance of 90%. However, a large fraction of the variability is due to the tides, which are not of interest in this study. Thus, further validation was carried out with the high water levels (HWL), i.e. the peak water levels at high tide.

The time-series of intramonthly 90% quantiles of the HWL were compared to observations for the tide gauges where long-term data sets are available. As an example, Fig. 4 shows the values as simulated (after correction) and observed, respectively, for the tide gauge in Cuxhaven. The represented variances, as well as the correlations of the simulated values for all tide gauges, are given in Table 1.

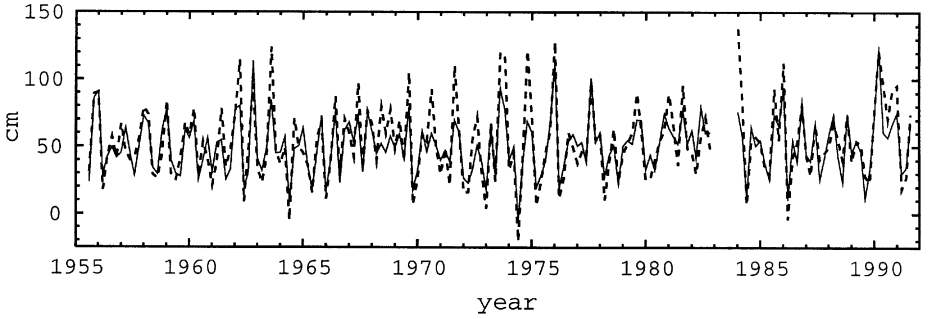

Fig. 4. Time-series of the 90% percentiles of intramonthly storm-related water level variations of Cuxhaven (in cm), as derived from in situ observation (dashed) and estimated from the dynamical model with correction (solid).

Table 1
Ability of the regression model (top) and the dynamical model (bottom) to reproduce observed intramonthly κ-percentiles. Listed are correlations and proportions of variance. The numbers are derived from independent data, i.e. disregarding the fitting period (1960–75) for the regression model

Quantile	Correlation				Explained variance			
	50%	80%	90%	97%	50%	80%	90%	97%
Smogen	0.85	0.84	0.80	0.71	72	70	62	50
Esbjerg	0.87	0.85	0.82	0.72	75	72	66	47
Cuxhaven	0.79	0.79	0.75	0.69	56	59	53	46
Delfzijl	0.78	0.79	0.75	0.70	57	59	57	49
Harlingen	0.81	0.81	0.77	0.71	64	64	58	50
Den Helder	0.77	0.80	0.77	0.68	57	63	59	45
H.v.Holland	0.67	0.71	0.70	0.59	37	47	47	31
Vlissingen	0.56	0.61	0.52	0.50	23	28	18	20
Esbjerg	0.79	0.80	0.79	0.71	62	61	58	37
Cuxhaven	0.88	0.86	0.87	0.86	74	72	74	71
Delfzijil	0.85	0.85	0.83	0.80	70	66	66	63
Harlingen	0.85	0.83	0.82	0.79	67	62	63	62
Den Helder	0.74	0.75	0.76	0.75	54	54	53	51
H.v.Holland	0.84	0.85	0.87	0.82	66	72	74	65
Vlissingen	0.65	0.71	0.74	0.78	35	23	23	40

The correction of model data is possible only for those stations along the coast where observed data are available. In general, the analysis is thus performed for the uncorrected model output; this tends to underestimate high percentiles and their linear trends (see Section 4). However, for rating the results of an increase in atmospheric carbon dioxide concentrations with the dynamical model, underestimated model results from the past are compared to equally underestimated model results from the scenarios, so that the significance of the resulting effects is not affected.

3.2. Statistical model

The verification of the model is performed for an independent period, by comparing observed intramonthly water level percentiles with the estimated values (Fig. 5). This comparison is achieved by two conventional measures of skill, namely the correlation skill score ρ_κ and the percentage of represented variance ε_κ for $\kappa = (50\%, 1), (50\%, 2)$ to $(97\%, 8)$ (Livezey, 1995):

$$\rho_\kappa = \frac{\text{Cov } (\hat{q}_{k;t}, q_{k;t})}{\sqrt{\text{Var } (\hat{q}_{k;t})\text{Var } (q_{k;t})}},$$

$$\varepsilon_\kappa = 1 - \frac{\text{Var } (\hat{q}_{kt} - q_{k;t})}{\text{Var } (q_{k;t})}, \tag{8}$$

where $\hat{q}_{k;t}$ is the estimated κ percentile in the month t.

The regression model (7) is used to estimate the water level percentiles for the years 1900–1959, 1976–1996. The in situ data for these years have not been used for the fitting of the regression model and thus represent independent evidence. The correlations and represented variances are listed in Table 1. The capability of the regression model is nearly as high as that of the dynamical model and, at some tide gauges (e.g. Esbjerg), even higher. This pattern indicates a very good correlation between monthly mean atmospheric pressure fields and the HWL percentiles, along the North Sea coast.

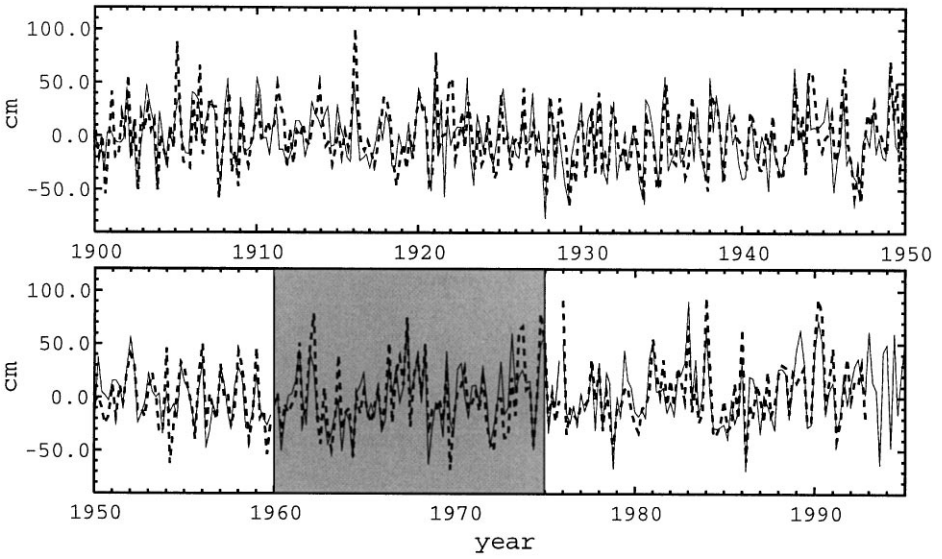

Fig. 5. Time-series of the 90% percentiles of intramonthly storm-related water level variations in Cuxhaven (in cm), as derived from in situ observations (dashed) and estimated from the monthly mean air-pressure field (solid). The fitting period is shaded.

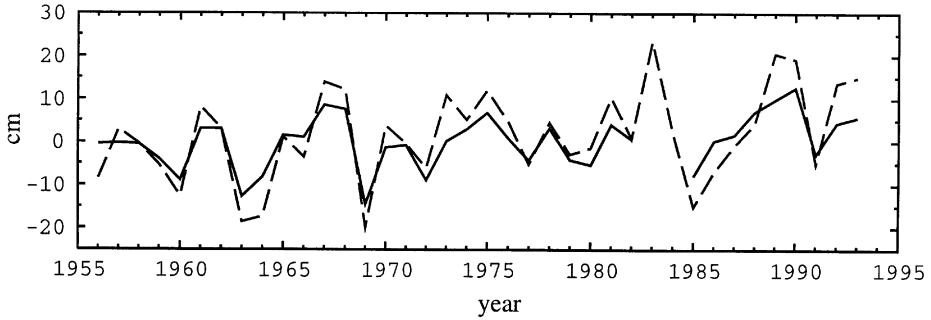

Fig. 6. Time-series of the anomalous winter mean (NDJFM) of the dynamical model (solid) and the 50% percentile of the statistical model (dashed) it Cuxhaven, for the winters 1955/56 –1992/93 (in cm). The correlation coefficient is 0.91.

In Fig. 6, the winter mean HWLs from the dynamical model are compared to the winter mean of the reconstructed intramonthly 50% quantiles. From the good agreement it can be concluded that the reconstructed 50% quantiles are a good proxy for the atmospherically forced monthly mean HWL. Their winter averages (NDJFM) are then treated in an analogous way to the HWL winter mean from the dynamical model; in the evaluation of the scenarios (Section 5).

4. Analysis of the past development

The analysis of the past development at the available tide gauges is carried out in parallel for the hindcast data and the in situ data. The investigation addresses the temporal variability (including trends) of winter mean high water levels (November–March) and high intramonthly percentiles.

In the case of the winter mean in situ data, the records exhibit upward trends which are, in part, unrelated to a change in meteorological conditions. Therefore, the analysis of the in situ data is restricted to the percentiles.

4.1. Dynamical model hindcast: 1955–1993

The 1955–93 trend in the HWL winter means, as well as in the 90% quantiles, is positive in the German Bight and Danish Coast and slightly stronger (up to 2 mm/yr) for the mean values (Fig. 7). Off the British Coastline, no decisive change (all values below 1 mm/yr) in HWLs is found. The intramonthly 95 and 97% quantiles behave much the same as the 90% quantiles (not shown).

In the hindcast results the meteorological forcing, i.e. atmospheric pressure and wind stress, is the only forcing variable, so that the simulated increase in the height of mean winter HWL must be due to changes in the low-frequency meteorological forcing.

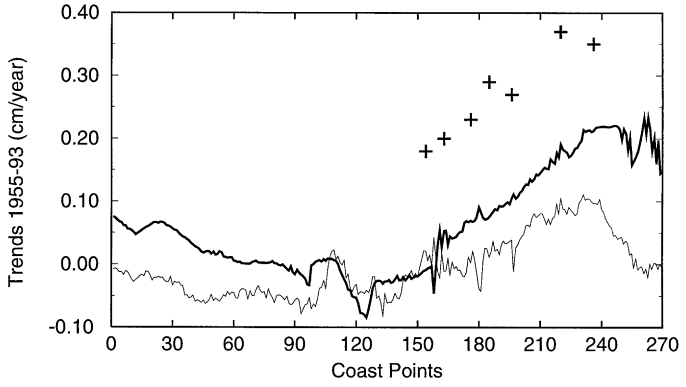

Fig. 7. Trends of uncorrected winter mean HWLs (in cm/yr), November–March (full line) and 90% quantiles (dashed line) of high tide sea levels, 1955–93. Statistically reconstructed winter mean HWL trends are given (as crosses), where available.

One possible explanation is a change in the prevailing mean atmospheric circulation. Indeed, the North Atlantic Oscillation Index (NAOI) has increased significantly since the 1960s. (Hurrell, 1995). To assess the link between NAO and the HWL winter mean along the North Sea coast, the time coefficient of the first EOF of HWL winter means was correlated with the NAOI for the time 1955–93 (the first EOF accounts for 76% of the HWL winter mean variance, at the 270 grid points around the North Sea). The resulting correlation coefficient of 0.58 indicates that the planetary scale circulation has only a moderate effect on the mean water levels in the North Sea.

Another possible explanation is related to the inverse barometric effect: under the assumption of an infinite and equilibrium ocean, a decrease of local air pressure of 1 hPa causes an increase of local sea level by 1 cm. We tested this explanation, by comparing the differences of the 5-year means 1988–92 and 1955–59 in SLP and HWL; it was found that the patterns were inconsistent with the hypothesis of an inverse barometric effect.

4.2. Statistical model reconstruction and observations: 1843–1992

Linear trends obtained from observations for the years 1955–92 (for comparison with the hindcast results) and for the past 100 years (for a longer perspective) are summarised in Table 2. The values representing the 39 years of simulation are positive at all of the tide gauges under investigation and for all the quantiles. The results obtained are also larger than those calculated from the hindcast, confirming the underestimation of the high percentiles by the numerical model, if not corrected. For the 100 year period, however, the trends are much smaller.

An indication of the relationship between the linear short- and long-term trends can be gained from Fig. 8. It shows the linear 39-year-trends for the years 1840–78, … , 1955–93 at the tide gauge of Cuxhaven. The most pronounced feature is a variation with an amplitude of some ± 0.35 cm/yr; this is one order of magnitude larger than

Table 2
Linear trends for the different percentiles and stations, for the periods 1955–93 and 1893–1993 (in cm/yr)

Period		1894–1993			1995–1993	
Quantiles	80%	90%	97%	80%	90%	97%
Smogen	0.02	0.03	0.03	0.24	0.31	0.25
Esbjerg	0.01	0	0.04	0.35	0.37	0.41
Cuxhaven	0.02	0.04	0.04	0.15	0.37	0.38
Delfzijl	0.05	0.07	0.07	0.27	0.49	0.56
Harlingen	0.08	0.16	0.20	0.23	0.41	0.54
Den Helder	0.06	0.10	0.16	0.18	0.36	0.31
H.v.Holland	0.03	0.04	0.05	0.15	0.26	0.26
Vlissingen	0.06	0.06	0.05	0.08	0.03	0.18

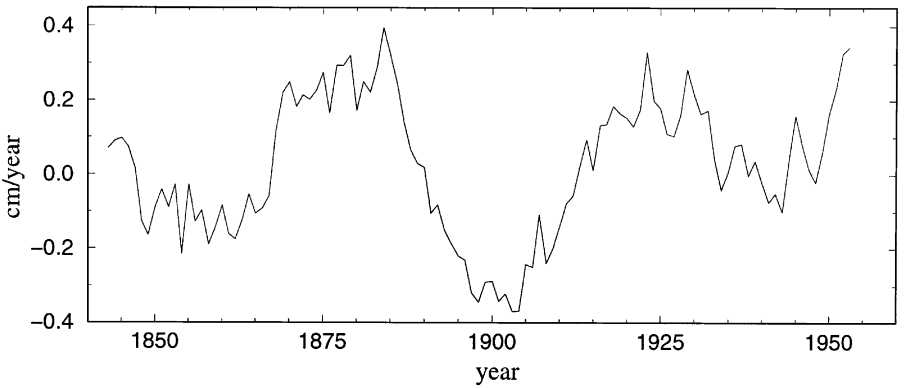

Fig. 8. Linear trends (in cm/yr) of intramonthly 90% quantiles of high water level for the winter, derived from running 39 year intervals of in situ data in Cuxhaven. On the horizontal axis, the year at the beginning of the 39-year interval is given i.e. "1850" refers to the interval 1850–1888.

the overall linear trend from 1843 to 1992 (which amounts to 0.039 cm/yr). Although, in recent years, the absolute value of the maximum exceeds that of the minimum, inspection of the whole period reveals no pronounced increase in the 90% quantiles within the last century.

The other tide gauges along the North Sea coast line – most of them with slightly shorter time series – qualitatively confirm this finding. From this evidence, the recent upward trend in storm surge intensities – even after subtraction of the mean values – is within the limits of previous variations.

The trends in mean HWLs are reconstructed by the statistical model in order to isolate the atmospherically forced effect. The results are shown in Fig. 7 for a direct comparison with the numerical model.

Finally, the NAO index was correlated with the longer time series of the statistically reconstructed 50% intramonthly percentile HWL, giving a correlation of 0.58 also for

the entire past century. However, the SLP pattern used in the reconstruction (cf. Fig. 3 (top)) is theoretically correlated to the NAOI ($\rho = 0.91$). Thus, the North Atlantic Oscillation determines–to some extent at least, the winter mean HWLs in the North Sea.

5. Analyses of the "$2 \times CO_2$" scenario

The ECHAM3/T106 time-slice experiments provide two scenarios, a control run with present day conditions and a "$2 \times CO_2$" run, simulating conditions at the expected time of doubled atmospheric CO_2 concentrations. 10 m wind and SLP fields from both scenarios were used as atmospheric boundary conditions for the numerical model the SLP fields were used as input data for the statistical model. In this way, two independent scenarios for the expected changes of storm-related water level variations along the coast of the North Sea are derived.

The two GCM runs were also compared with respect to mean SLP, in order to estimate the possible inverse barometric effect. Over the North Sea, an increase of sea level pressure of about 4 hPa in the "$2 \times CO_2$" scenario was found, so that an increase of up to 4 cm in the mean sea level is possibly attributable to this effect.

5.1. Dynamical model

The differences in simulated winter mean HWL, between "$2 \times CO_2$" run and control run, are shown as solid line in Fig. 9. For comparison, an estimated ± 2 standard deviation band, derived from all 5-winter means within the *39*-year hindcast (i.e. 55–59, 56–60, etc.), is indicated by shading.

Here, the differences exceed twice the standard deviation from the past in most positions around the North Sea. However, variability of the 5-winter-mean HWL is fairly low, so that even rather small changes give a significant effect: the analysis presented here suggests an increase in mean HWL, due to doubled carbon dioxide concentration in the atmosphere, of the order of 5–10 cm.

The expected change of the 90% quantiles (after subtraction of the winter mean HWLs) is presented in Fig. 10. Although the past variability is even smaller than that of the five winter means, the difference between the climate scenarios is only on the order of one standard deviation of the variations in the past 39 years. Thus, the simulated change in the 90% percentile may be due to the internal variability of the system "Atmosphere – North Sea" and unrelated to anthropogenic climate change.

Additionally, the dynamical model results for the corrected values at the tide gauges are given in Table 3. Agreement with the statistical model results is good, confirming the above-mentioned conclusion for the corrected values (cf. Section 5.2).

5.2. Statistical down-scaling

The simulated change in mean air pressure is fed into the regression model (7) and, hereby, an estimate of plausible future changes in high water level variation statistics at the eight considered tide gauges is obtained.

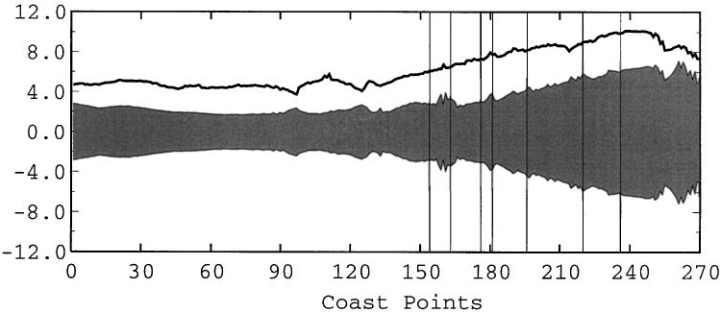

Fig. 9. (a) Black line: Difference of the 5-winter-mean of high water levels in the "$2 \times CO_2$" and the control run (in cm) (b) shaded: Band of 2 standard deviations of 5-winter-mean high water levels, as derived from the hindcast 1955–93, and (c) vertical lines: tide gauge positions.

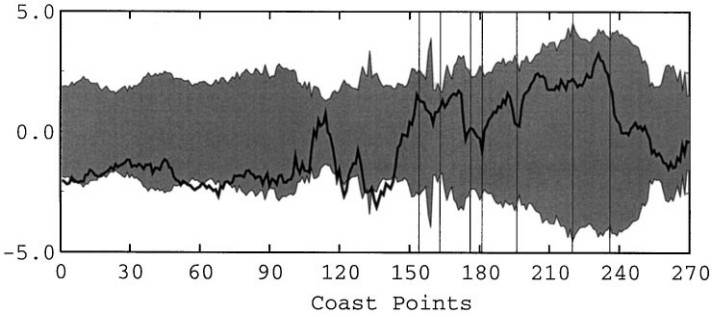

Fig. 10. (a) Black line: Difference of the intramonthly 90% quantiles of high water levels in the "$2 \times CO_2$" and the control run (in cm) (b) shaded: Band of 2 standard deviations of the intramonthly 90% quantiles of high water levels, as derived from the hindcast 1955–93; and (c) vertical lines: indicate gauge positions.

Table 3
Expected changes of future storm-related water levels for the different stations and percentiles for the winter (NDJFM), under the conditions of the "T 106 time-slice experiment". (in cm.). Left: statistical model; right: dynamical model (including corrections)

Quantile	Statistical model				Dynamic model			
	50%	80%	90%	97%	50%	80%	90%	97%
Smogen	6	6	6	7	—	—	—	—
Esbjerg	9	12	14	16	11	13	10	13
Cuxhaven	9	12	15	20	8	10	12	13
Delfzijl	7	11	14	17	8	9	9	15
Harlingen	8	11	13	16	9	9	7	10
Den Helder	6	8	11	12	8	7	8	8
H.v.Holland	5	7	8	9	6	6	7	11
Vlissingen	4	5	5	8	5	5	7	9

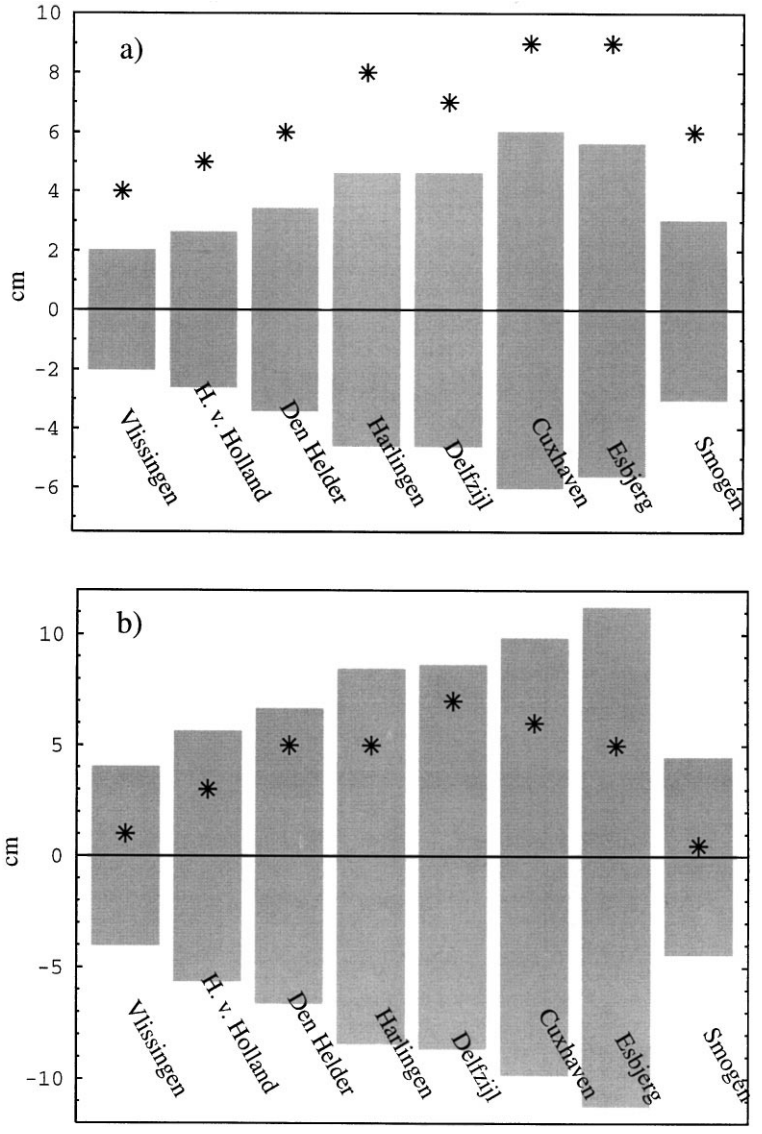

Fig. 11. (a) 5-winter-mean of high water level (~50% percentile of the $2 \times CO_2$ scenario (stars) and estimated variability ($\pm$ two standard deviations) of all 5-winter-means (grey), from 1900 to 1996; and (b) the same as (a), but for the 90% percentile (reduced by mean). (in cm)

This procedure provides the results presented in Fig. 11. The two graphs are set up in the same manner as Fig. 9 and 10, i.e. the winter mean HWL (a) and the difference between winter mean and 90% quantiles (b) are treated separately. The tide gauges where data are available are marked in Figs. 9 and 10, by the vertical lines.

The combined results are presented in Table 3, using the corrected dynamical model results. For all the tide gauges, dynamical and statistical model alike, the difference between the scenarios tends to be highest for the highest percentiles. Thus, the distribution of HWLs does not only shift to higher values, but it also broadens. The change amounts to 1–2 dm, with the highest values associated with the German Bight.

6. Discussion and comparison

In the previous Sections, two ways of hindcasting the past climate and processing GCM climate scenarios were presented, validated and evaluated. However, it is the combination of the results that gives the most comprehensive insight into the processes.

In the past, it has been shown that positive trends are indeed present in both the simulated and observed data – when only rather short periods of time on the order of 30 or 40 years are regarded. Examining longer time-series from the data, however, somewhat changes the interpretation: the trends no longer appear to be linear, but a strong decadal (or even longer) variability overrules a negligible long-term trend. Thus, trends from only 40 years of data cannot be regarded as good indicators of any long-term climatic change.

Regionally, the North Sea coastline is divided into two distinct areas. The British coast-line is mostly unaffected by change; however along the European continent, the past decades have been a time of increasing mean as well as extreme sea levels (but not to an unusual extent in relation to earlier decades).

The climate change scenarios provide data for only six years and given the variability in the past that renders even a 39 year time-series of only limited value are not very reliable predictors of future climate. However, at present they are the best estimates available and are used, therefore, to provide an initial estimation and to establish a methodology that can be used for future longer-term scenarios.

From the analysis of the climate scenarios, the following results emerge: (a) the mean high tide water level increases by about three standard deviations from the 39-year hindcast, amounting to some 10 cm and (b); the distributions additionally broaden (in terms of the 90 and 97% quantiles), but only on the order of 1–2 standard deviations of the anomalies of the 39 year hindcast (around 5–10 cm).

The spatial distribution of this rise in mean HWLs is in accordance with the 1955–93 trend in the winter mean HWL, suggesting that the differences between the two scenarios might be an extension of the trends found for the past. For the wave climatology in the northeastern Atlantic, Gunther et al. (1998) have found a similar result, using the same GCM data as forcing for their wave model.

If the NAO was indeed responsible for the trends in the hindcast, as suggested in Section 4, this would imply that an increase of CO_2 concentrations in the atmosphere might be correlated with slow changes in the North Atlantic Oscillation; these in turn, could result in a slight increase in mean water levels in the North Sea. However, with only six years of time-slice scenarios available, it is too early to form such a conclusion.

It was shown that the empirical model, simple as it is, predicts consistently similar to the dynamical model, although it is fed only with the relationship between two parameters – monthly averaged SLP-field and water levels – from the past. The dynamical model, on the other hand, is believed to account for changes in the dynamics of the system as well as changes in the strength of one parameter that has been identified as decisive in the past.

The above consistency is an indication that a large increase of CO_2 concentrations in the atmosphere will not lead to dramatic changes in the circulation, but that the same mechanisms – if possibly with a slightly different strength – will remain in operation. Based upon data analysis for the past and a down-scaling technique for the climate change scenarios (once again, for the ECHAM3/T106 run), Schmith et al. (1997) have come to the same conclusion.

Methodologically, the accordance between the statistical and the dynamical model output implies that future scenarios, as well as presently available coarse resolution predictions can more reliably be investigated with the much less expensive empirical model. Thus, a rather rapid approach to down-scaling GCM results – for one parameter and a restricted area – is gained.

7. Conclusions

Several conclusions, with regard to different scientific questions posed, can be drawn from the exercise that has been presented.

Firstly, the 39 years of data (from 1955 to 93) were investigated extensively with respect to sea level variability and placed within a long-term perspective, by comparison with observations and reconstructions from the statistical model. It was found that variability on time-scales as short as 40 years is an order of magnitude larger than that observed over 100 years. With such a high amount of noise, the diagnosed short-term trends are not identifiable as anthropogenically induced. However, the past 40 years were indeed a period of increasing water levels – storm related as well as mean – if not exceptionally strong. Mean high tide water levels rose by some 0.1–0.35 cm/yr, the intramonthly 97% quantiles increased additionally by up to 0.4 cm/yr, depending upon the location of the tide gauge. Changes of this order have, also been observed, however, earlier in this century.

Secondly, the changes in mean and extreme sea levels that are to be expected for a climate regime with an enhanced "Greenhouse Effect" were analysed according to the ECHAM3/T106 scenario. Both effects have been regarded separately and each amounts to an increase on the order of one decimeter. In relation to the variability that has been simulated for the years 1955–93, this increase can be expressed as three standard deviations of the same entity for the mean sea levels and 1–2 standard deviations for the 90% quantiles.

Thirdly, the pattern of change in the sea levels along the North Sea coast due to doubled carbon dioxide concentration in the atmosphere is quite similar to the pattern of the trend in the past 39 years. This pattern might mean that a distinct change in the forcing is responsible for just this pattern, similaly that this distinct

change has occurred in the past and will extend into the future in a condition of increasing atmospheric CO_2 concentrations. However, this aspect cannot be decided upon with the short-term scenario data that are presently available.

As a fourth point, the accordance of the statistical and the dynamical model can be interpreted as an indication that the dynamics of the system do not change decisively in the case of doubled carbon dioxide concentrations in the atmosphere. If the dynamics did indeed change, then the statistical link between two parameters, namely the monthly mean sea level pressure fields and the elevations along the North Sea coast, would be expected to break down in the "$2C_2$" scenario; in contrast, the dynamical model output ought to be able to react flexibly. That both models behave similar is, thus, an indication towards rather stable conditions.

The latter three points, regarding the possible development of the storm surge climate under a regime of doubled carbon dioxide concentrations in the atmosphere, depend critically upon the validity of the ECHAM3/T106 scenarios. The statistical model has also been applied to a 30 year experiment with a coarser (T42) resolution, resulting in nearly no change due to increased atmospheric carbon dioxide concentrations. Therefore, at least part of the evaluation ought to be repeated, when longer-term data are available-so that confidence in the results is enhanced.

Finally, the consistency between the statistical and dynamical model outputs provides a helpful methodological insight. If there is no dramatic change in the dynamics and the statistical model performs satisfactorily, then future scenarios (as well as present long term but coarse resolution scenarios) can be processed much faster and with reasonable confidence.

Acknowledgements

The authors are grateful to Lennart Bengtsson, Max-Planck-Institut Hamburg, for providing the ECHAM3/T106 scenarios and to Matthias Dorn and Andre Hufschmidt for help with the data. Joachim Dippner and John de Ronde helped us to access the water level data.

The work presented in this paper was funded by the German Ministry for Education, Science, Research and Technology (BMBF) under the contract number 03F0141B.

References

Backhaus, J.O., 1985. A three-dimensional model for the simulation of shelf sea dynamics. Deutsche Hydrographische Zeitschrift 38, 165–187.

Beersma, J., Rider, K., Komen, G.J., Kaas, E., Kharin, V., 1997. An analysis of extra-tropical storms in the North Atlantic region as simulated in a control an $2 \times CO_2$ time-slice experiment with a high resolution atmospheric model. Tellus 49A, 347–361.

Bengtsson, L., Botzet, M., Esch, M., 1995. Hurricane-type vortices in a general circulation model. Tellus 47A, 175–196.

Cubasch, U., Hasselmann, K., Hoeck, H., Maier-Reimer, E., Mikolajewicz, U., Santer, B.D., Sausen, R., 1992. Time-dependent greenhouse warming computations with a coupled ocean-atmosphere model. Climate Dynamics 8, 55–82.

Cubasch, U., Waskewitz, J., Hegerl, G.C., Perlwitz, J., 1995. Regional climate changes as simulated in time-slice experiments. Climatic Change 31, 273–304.

Cubasch, U., von Storch, H., Waskewitz, J., Zorita, E., 1996. Estimates of climate change in Southern Europe using different downscaling techniques. Climate Research 7, 129–149.

Damm, P., 1989. Klimatologischer Atlas des Salzgehaltes, der Temperatur und der Dichte in der Nordsee, 1968–1985. Institut fur Meereskunde der Universitat Hamburg, Technical Report, 6–89, pp. 1–81.

Flather, R.A., Smith, J., 1998. First estimates of changes in extreme storm surge elevations due to doubling of CO_2. The Global Atmosphere and Ocean System (in press).

Führböter, A., Jensen, J., Schulze, M., Toppe, A., 1988. Sturmflutwahrscheinlichkeiten an der deutschen Nordseeküste nach verschiedenen Anpassungsfunktionen und Zeitreihen (in German). Die Küste 47, 163–186.

Günther, H., Rosenthal, W., Stawarz, M., Carretero, J.C., Gomez, M., Lozano, I., Serrano O., Reistad, M., 1998. The wave climate of the Northeast Atlantic over the period 1955–1994: the WASA wave hindcast. The Global Atmosphere and Ocean System (in press).

Hainbucher, D., Backhaus, J.O., Pohlmann, Th. 1987. Transport of conservative passive tracers in the north sea: first results of a circulation and transport model. Continental Shelf Research 7 (10), 1161–1179.

Hurrell, J.W., 1995. Decadal trends in the North Atlantic Oscillation: regional temperature and precipitation. Science 269, 676–679.

Kochergin, V.P., 1987. Three dimensional prognostic models. In: Heaps, N.S. (Ed.), Three dimensional Coastal Ocean Models. American Geophysical Union, Washington, DC. (Coastal and Estuarine Science, 4), pp. 201–208.

Livezey, R.E., 1995. The evaluation of forecasts. In: von Storch, H., Navarra, A. (Ed.), Analysis of Climate Variability: Applications of Statistical Techniques. Springer, Berlin, pp. 177–196 (ISBN 3–540–58918-X).

Luthardt, H., Hasse, L., 1983. The relationship between pressure field and surface wind in the German bight at high wind speeds. In: Sundermann, J., Lenz, W. (Eds.), North Sea Dynamics. Springer, Heidelberg, pp. 340–348.

Orlanski, I., 1976. A simple boundary condition for unbounded hyperbolic flows. Journal of Physical Oceanography 12.

Pohlmann, T., 1996. Predicting the thermocline in a circulation model of the north sea – Part I: model description, calibration and verification. Continental Shelf Research 16, 131–146.

Rohde, H., 1992. Die Veränderung der Scheitelhöhen hoher Sturmfluten in Hamburg (in German). Die Küste 53, 225–239.

de Ronde, J.G., de Ruijter, W.P.M., 1987. Die Auswirkungen eines verstarkten Meeresspiegelanstiegs auf die Niederlande. Die Küste 45, 124–163. (in German)

Schmith, T., Kaas, E., Li, T.-S., 1997. Northeast Atlantic storminess 1875–1995 re-analysed. Climate Dynamics, in review.

Smith, S.D., Banke, E., 1975. Variation of the sea surface drag coefficient with wind speed. Quaterly Journal of the Royal Meteorological Society 101, 665–673.

Tomczak, G., Goedecke, E., 1962. Monatskarten der Temperatur der Nordsee, dargestellt für verschiedene Tiefenhorizonte. Deutsche Hydrographische Zeitschrift Erg.-H. (B) Nr.7, 112 S. (in German)

Trenberth, K.E., Paolino, D.A., 1980. The Northern Hemisphere sea-level pressure data set: trends, errors and discontinuities. Monthly Weather Review 108, 855–972.

Tyler, D.E., 1982. On the optimality of the simultaneous redundancy transformations. Psychometrika 47, 77–86.

von Storch, H., Frankignoul, C., 1997. empirical modal decomposition in coastal oceanography. - the sea. The Global Coastal Ocean: Processes and Methods, vol. 10, Wiley, New York, pp. 419–455 (in press).

von Storch, H., Reichardt, H., 1997. A scenario of storm surge statistics for the German Bight at the expected time of doubled atmospheric carbon dioxide concentration. Journal of Climate 10, 2653–2662.

von Storch, H., Zwiers, F.W., 1998. Statistical Analysis in Climate Research. Cambridge University Press, Cambridge (in press).